Early Prediction of Lithium-Ion Battery Cycle Life by Machine Learning Methods

Ankan Mitra, Arizona State University
Rong Pan, Ph. D., Arizona State University

Key Words: feature selection, ensemble machine learning, support vector regression, degradation, reliability prediction

2022 Annual Reliability and Maintainability Symposium (RAMS) | 978-1-6654-2432-5/22/$31.00 ©2022 IEEE | DOI: 10.1109/RAMS51457.2022.9893916

SUMMARY & CONCLUSIONS

For a lithium-ion battery, its cycle life is defined as the number of full charge cycles that a battery can undergo until its full charge capacity falls below 80% of the design capacity. In a recent study by Severson et al. [1], a large set of lithium-ion battery cycle life experiments were conducted and analyzed, and early cycle data were used to predict battery lives without any prior assumptions on degradation mechanism. In this paper, we reexamine the data and suggest additional features to the model, which also use early cycle data (up to the first 100 cycles), for a better battery cycle life prediction. We suggest an ensemble machine learning method that combines several classifiers such as the k-nearest neighbor classifier, neural networks, support vector machines and decision tree-based classifiers for classifying batteries to low or high lifetime category. It is found that our ensemble approach provides more robust predictions. For predicting cycle life, a support vector regression model is suggested, and we compare it with an elastic net-based regression model. It is found that SVR outperforms elastic net in terms of percentage prediction error.

1 INTRODUCTION

Lithium-ion battery is the most common type of rechargeable batteries in portable electronics, electric vehicles, military/space applications. These batteries generally have long lifetime (in terms of the number of charge-discharge cycles), often lasting several months to years. With a high cycle life, performing a field failure-based performance improvement becomes counter-productive. Degradation of the performance of a battery can be observed over time to predict when the performance of the battery will become below standard, which can be regarded as a battery failure. This type of failure is called soft failure [2]; that is, the actual component may still be in usable condition, but it is not at par with the industry recommended minimal performance level. The degradation of a lithium-ion battery is measured by the reduction of the maximum capacity of a charge that a battery can hold at a time. An FMEA study of lithium-ion batteries [3] revealed that chemical and mechanical changes in the electrodes over the life cycle of a battery caused the reduction in battery capacity. The industry standard defines a quantitative term, “cycle life”, to quantify the number of full charge cycles a battery can undergo until the full charge capacity of battery falls below 80% of its design capacity.

It is known that the degradation mechanism of a lithium-ion battery may vary with the amount and intensity of battery use as well as its charging conditions. Hence, it is of practical importance to be able to predict the cycle life of a battery from its earlier cycle data. This predictive analysis is not only helpful for manufacturers to improve battery design, but also for customers to have an accurate battery life estimation based on its usage. In this study, multiple sets of lithium-ion battery life testing data are analyzed, and early cycle data are used to predict the cycle lives of batteries. We consider some new temperature and voltage curve-based features and use an ensemble machine learning (EML) approach to build a powerful predictive model.

This paper is organized into four sections hereafter: Section 2 describes the dataset and explains different features used in the model. Section 3 analyzes the importance of these features and uses them to build classification and regression models. Section 4 presents our classification and regression prediction results and compares them with the results from a previous study. Finally, Section 5 concludes the paper.

2 DATA DESCRIPTION

The entire dataset is available in the github repository, https://data.matr.io/1/projects/5c48dd2bc625d700019f3204. This dataset contains information about commercial grade Lithium Iron Phosphate (LiFePO) cells and has been compiled by Severson et. al. [1]. All the battery cells in the dataset have a nominal capacity of 1.1 Ah. There are 3 test batches (each of them was tested on a different date) with 41, 43 and 40 battery cells (a total of 124) in each batch, respectively. All cells were charge-discharge cycled in a temperature-controlled chamber with various fast charging conditions, starting from 3.6 C to 6 C, which was deemed to be an extreme fast charging condition. The descriptions of some charging variables included in the dataset are given below:

1. cycle-life: the number of full charge cycles that a battery can undergo until the full charge capacity of the battery falls below 80% of its design capacity.
2. charge-policy: “C1-Q1-C2” - C1 and C2 represent the first and second applied current in amount of coulomb of charge flow per second, and Q1 is the percentage state-of-charge

978-1-6654-2432-5/22/$31.00 ©2022 IEEE

(SOC) at which the current is changed from C1 to C2. C2 charge is applied till to 80% SOC. After that, all batteries are charged in the same way: at 1 C of constant current till to 3.6 V, and then at a constant voltage of 3.6 V.

3. summary of cycles:
   (a) IR: internal resistance of the battery in each full charge cycle.
   (b) QC: charge capacity of the battery after a full charge cycle.
   (c) QD: discharge capacity of the battery after a full charge cycle.
   (d) Tavg: average temperature of the battery during a full charge cycle.
   (e) Tmin: minimum temperature of the battery during a full charge cycle.
   (f) Tmax: maximum temperature of the battery during a full charge cycle.
   (g) chargetime: time to charge the battery in a full charge cycle.
4. cycle data (for each full charge cycle)
   (a) I: current monitored over time.
   (b) Qc: charge capacity of the battery over time
   (c) Qd: discharge capacity of the battery over time
   (d) T: temperature of the battery over time
   (e) V: voltage (potential) of the battery over time

To better understand the dataset, we plot the following histograms for Batches 1-3 to show the distributions of cycle life of the battery cells in these batches. Such variational cycle lives are obtained because of the varying fast charging conditions. See Figure 1.

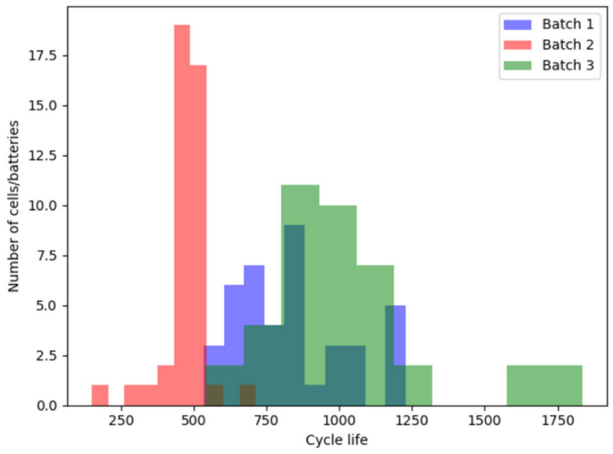

Figure 1. Histograms of battery cycle lives

Figure 2 shows some battery cell characteristics such as (a) temperature of cell, (b) discharge capacity of cell, and (c) charging time over full charge cycles for the cells from the frist batch. The variation in the temperature of battery (see Figure 2(a)) comes from a combined effect of charging condition and the internal energy and resistance of the cell. As observed from Figure 2(b), the discharge capacity of each cell starts fading exponentially after a certain point, indicating significant degradation. Also seen from Figure 2(c), the charge time increases as the discharge capacity fades more [4]. However, from (b) and (c) one can also observe that at early cycles (up to the cycle life of 100) the capacity degradation is very small, almost undetectable on most cells.

We notice that these plots do not reveal how much discharge capacity or temperature varies within a single full charge-discharge cycle for each cell. It is clear to see that the more the number of charge-discharge cycles a cell undergoes, the more the capacity degradation happens. Therefore, the variation of these properties within each cycle can be important for cycle life prediction. Figure 3 shows the variation of temperature curves as the number of full charge cycles increases for three different cells.

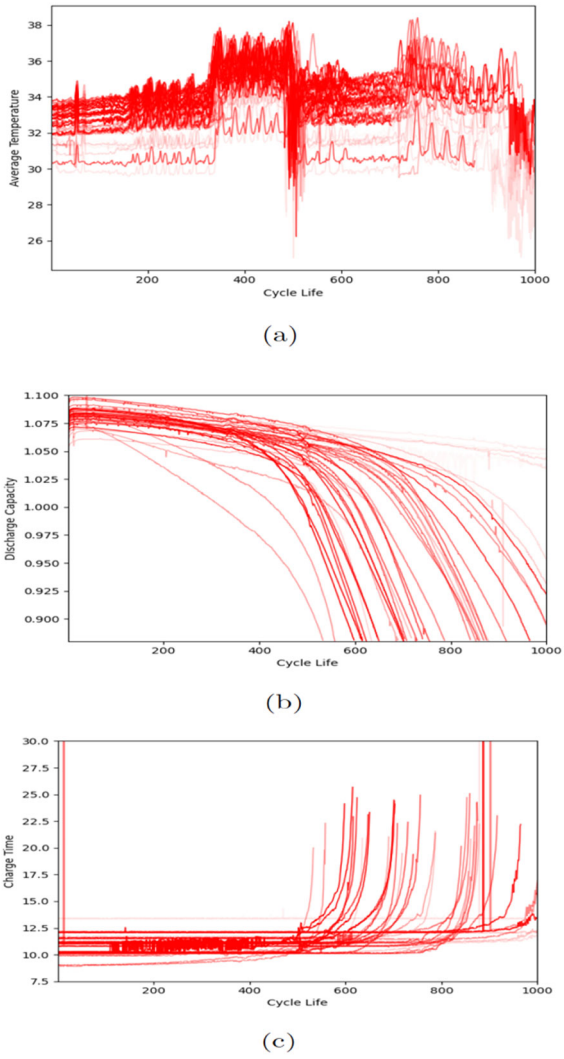

Figure 2. Some characteristics of cells in Batch 1

Clearly, within a cycle the variation of temperature can reveal something about the cycle life. Not only is the minimum or maximum temperature within a cycle important, but also how the temperate variation changes (progresses) along the time matters too.

Another performance characteristic is the variation in the curves of the discharge capacity or temperature over voltage

within each charge cycle (they are not shown here due to the page limitation). These variations in curves, particularly at early cycles, can be more informative than the maximum discharge capacity or the average temperature for predicting cell degradation. This gives a basis for the creation of additional features that might help in predicting the cycle life of battery cell.

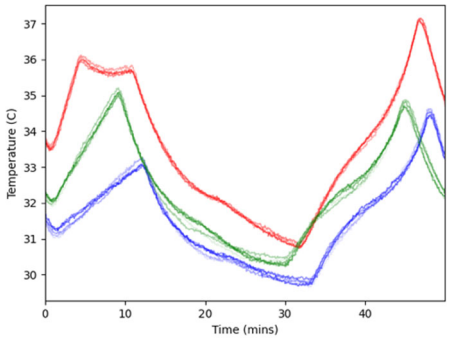

(a) Cycles 1 to 5

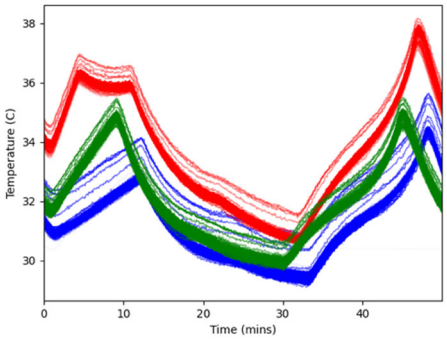

(b) Cycles 10 to 100

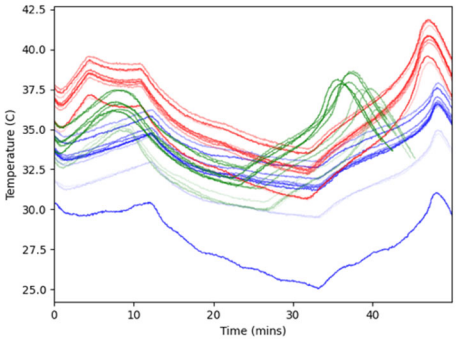

(c) Cycles 300 to 500

Figure 3. Temperature variation in 3 cells from Batch 1

The next section will outline the machine learning (ML) approach considered in this study. Overall, we will conduct two ML tasks: one is to classify a battery cell to a "high" or "low" lifetime category and the other one is to predict the cell's (soft) failure time. First, we define several features that may potentially affect the cycle life. In the work done in [1], several of these features are already considered, abut in our study, some additional features based on the temperature and voltage curves within each charge cycle are proposed. Also different from [1], we proposed an ensemble approach for the classification task and a support vector regression (SVR) model for the regression task.

3 *DATA ANALYSIS*

The goal of this study is to predict the cycle life of battery cell by using only its earlier cycle data. We classify batteries to either "low lifetime" or "high lifetime" category. This classification can be immensely useful to both manufacturers and customers. As the lifetime of a lithium-ion cell is expected to be long, so a product design engineer would like to know what faulty designs may cause a cell to be of "low lifetime". On the other hand, for a customer, an accurate estimation of a battery's cycle life based on its earlier life behavior and its use profile will allow the customer to adopt proper maintenance schedule and avoid catastrophic failure. Most systems nowadays are equipped with advanced sensors, which make it possible to monitor various battery properties throughout its use period [5-7].

3.1 *Feature Definition and Feature Importance*

The features being considered in our study are listed in Table 1. Some of them are taken from [1], but based on the discussion in Section 2, we also derive many new features (shown in bold font). For example, the features X4 to X6 are derived from the temperature-voltage curve with the formula: $\Delta T_{100-10}(\vec{V}) = T_{100}(\vec{V}) - T_{10}(\vec{V})$.

In order to classify battery cells to "high" or "low" lifetime category, we first define a threshold value of 550 cycles. That is, a cell with cycle life of more than 550 cycles is classified as "high lifetime" and otherwise "low lifetime". We assign value 1 to "high lifetime" and 0 to "low lifetime".

Next, we screen these features based on their feature importance measures. For a regression task, an F score (Pearson's correlation coefficient for regression coefficients) for each individual feature can be calculated. If the feature has a statistically significant effect on the response variable, which is the cycle life, then this F score is high. For a classification task, this F score corresponds to the feature's ability to distinguish two different categories.

3.2 *Classification Task*

We choose an EML classification method because the ensemble approach is typically more robust to classifier-specific errors and can often give better predictions. There are five classifiers used in EML: Multi-Layer Perceptron (MLP) Classifier, K-Nearest Neighbors (KNN) Classifier, Support Vector Machine (SVM), Random Forest (RF) and AdaBoost Classifiers. The strategy used for selecting the best hyperparameters for each model is shown in Figure 4. Following [1], the whole dataset is partitioned to a training set of 41 cells, a primary test set of 43 cells, and a secondary test

set of 40 cells. The ensemble classifier's accuracy scores are reported for the primary and secondary test sets. For the training set, a cross-validated generalized accuracy score is reported. The ensemble classification strategy is a majority voting strategy, where a case is classified to the category that most of individual classifiers have voted it to. Only those important features listed in Table 1 are used in the classification task.

Table 1. Features and feature importance (unimportant features, as indicated by high p-values, are colored in red)

	Features	Symbol	Classification		Regression	
			F Score	p-value	F Score	p-value
$\Delta Q_{100-10}(V)$	Minimum	X_1	73.795	0.000	147.858	0.000
	Variance	X_2	42.561	0.000	65.952	0.000
	Mean	X_3	66.066	0.000	140.575	0.000
$\Delta T_{100-10}(V)$	**Minimum**	X_4	2.175	0.143	5.349	0.022
	Variance	X_5	3.119	0.080	3.191	0.077
	Mean	X_6	24.628	0.000	9.000	0.003
Discharge Capacity fade curve features	Slope of linear fit of Qd curve (2-100)	X_7	5.204	0.024	10.296	0.002
	Intercept of linear fit Qd curve (2-100)	X_8	0.706	0.402	3.267	0.073
	Slope of linear fit of Qd curve (91-100)	X_9	12.864	0.000	17.241	0.000
	Intercept of linear fit of Qd curve (91-100)	X_{10}	8.232	0.005	12.076	0.001
	Slope of linear fit of Qd curve (10-100)	X_{11}	4.747	0.031	9.828	0.002
	Intercept of linear fit of Qd curve (10-100)	X_{12}	0.734	0.393	3.448	0.066
	Discharge capacity of cycle 2	X_{13}	0.266	0.607	1.595	0.209
	Discharge capacity of cycle 100	X_{14}	2.107	0.149	2.448	0.120
Temperature - time curve-based features	**Area under temperature time curve (70-100)**	X_{15}	274.789	0.000	123.865	0.000
	Slope of area under temperature time curve (70-100)	X_{16}	8.100	0.005	2.477	0.118
	Intercept of area under temperature time curve (70-100)	X_{17}	276.885	0.000	134.744	0.000
	Maximum temperature (2-100)	X_{18}	6.393	0.013	10.515	0.002
	Minimum temperature (2-100)	X_{19}	47.520	0.000	45.504	0.000
Temperature - voltage curvebased features	**Area under temperature voltage curve (10-100)**	X_{20}	0.734	0.393	0.248	0.619
	Slope of area under temperature voltage curve (10-100)	X_{21}	1.731	0.191	2.972	0.087
	Intercept of area under temperature voltage curve (10-100)	X_{22}	0.379	0.539	0.023	0.881
Internal resistance based features	Internal resistance of cycle 2	X_{23}	12.333	0.001	24.235	0.000
	Minimum internal resistance (2-100)	X_{24}	14.337	0.000	27.190	0.000
	Change in internal resistance (2-100)	X_{25}	5.700	0.019	11.863	0.001
Other	Average charge time over first 5 cycles	X_{26}	12.870	0.000	24.523	0.000

3.3 *Regression Task*

For the regression task, two regression models are used: elastic net and support vector regression. Again, we only use the features that are identified to be significant in Table 1. We compare the elastic net-based model (as suggested by [1]) with the SVM-based regression model.

Elastic net is a linear-regression model which includes both L1 and L2 regularization terms, with parameters which can control both the regularization terms. The objective is to minimize the loss function given by:

$$Min_w \frac{1}{2n}|Xw - y|_2^2 + \alpha\rho|w|_1 + \frac{\alpha(1-\rho)}{2}|w|_2^2 \qquad (1)$$

where α and ρ are parameters to control the extent of L1 and L2 regularization. Both the regularization techniques together control the sparsity and overfitting of the fitted linear function.

Support vector machines use the concept of hyperplanes ($Xw = y$) and support vectors (points which are closest to the hyper-plane on both sides). The hyperplane defines the regression function, $y = f(x)$. However, SVM is not only restricted to classification tasks or linear hyperplanes. SVM for regression uses the same idea to find a good decision boundary, which could be linear or non-linear, and the boundary itself becomes the regression function fitted to the data. The objective function is as given below:

$$Min_{w,b,k_1,k_2} \frac{1}{2}w^T w + c\sum_{i=1}^{n}(k_1 + k_2) \qquad (2)$$
$$subject\ to: y_i - w^T\phi(x_i) - b \le \epsilon + k_1$$
$$w^T\phi(x_i) + b - y_i \le \epsilon + k_2$$
$$k_1, k_2 \ge 0$$

The transformation of features, $\phi(x)$, is related to a kernel function, $K(x_i, x_j) = \phi(x_i)^T\phi(x_j)$. This problem is solved optimally owing to the nature of the problem (convex programming), by using Karush-Kuhn-Tucker (KKT) conditions. Using KKT conditions, the dual coefficients (α's) are calculated for each data point in the problem. The final prediction is achieved by using those dual values along with the kernel function as shown below:

$$f(x) = w_0 + \sum_{i=1}^{n} \alpha_i y_i K(x_i, x) \quad (3)$$

It should be noted that in the solution process $\phi(x)$ is always calculated as an inner product (in the form of kernel function) and never used alone. Several kernel functions can be used for a linear or nonlinear transformation of the feature space, such as the polynomial kernel ($K(x_i, x_j) = (1 + x_i^T x_j)^m$), gaussian kernel ($K(x_i, x_j) = \exp(-|x_i - x_j|^2 / 2\sigma^2)$), hyperbolic kernel ($K(x_i, x_j) = \tanh(\beta x_i^T x_j - \delta)$), etc. These kernel transformations correspond to nonlinear features in the original feature space, but they become linear features in the transformed feature space. Specifically, the gaussian kernel (also known as radial basis function) transforms the original features into an infinite number of transformed features, without explicitly specifying these infinite number of features. Therefore, SVMs are often quite powerful and, with proper tuning, can provide very accurate decision boundaries.

A similar test strategy as used in the classification task is employed in this regression task. We train both regression techniques with 3 models: a model with top 7 features based on F score (Model 1), a model with features having p-value less than 0.1 (Model 2), and a model with all features (Model 3).

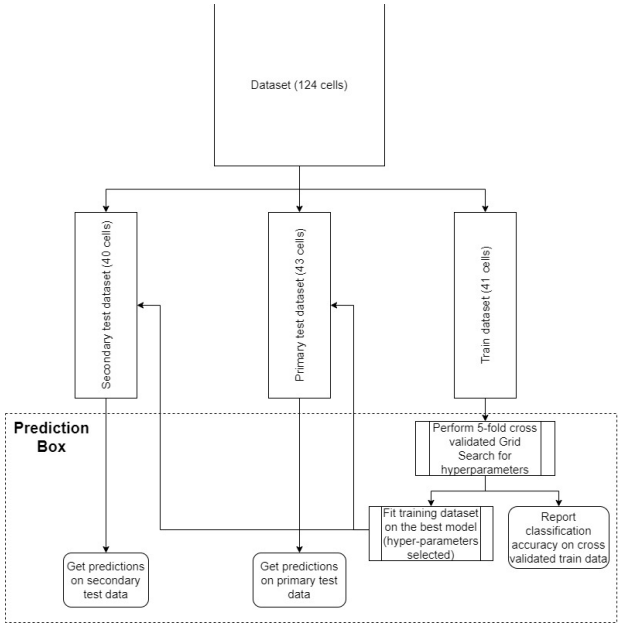

Figure 4. Strategy for model building and prediction

4 RESULTS AND DISCUSSIONS

Our models were developed in Python 3.7, with the scikit-learn package [8] for machine learning, on a laptop with 16GB of RAM.

Our ensemble approach to the classification task performs equally well as in Severson et. al. [1] on the same dataset partition scheme, and it has a classification accuracy of 97.5% on the secondary test set. However, the dataset partition scheme used by the other authors used the whole third batch data as the secondary test set. In order to remove any possible biases in the model to be developed, we randomize the data partition while maintaining the same number of cases in each set (i.e., 41, 43 and 40 cases, respectively). Our model is able to achieve equally well accuracy in several random partitions of data (even in imbalanced test sets). This shows that the ensemble approach to classification can achieve a performance that is not biased by the quantity of differently labeled data in a dataset.

Table 2. Classification accuracy scores

Model	Classification accuracy		
	Train	Primary test	Secondary test
1) Variance classifier [1]	82.1	78.6	97.5
2) Full classifier [1]	97.4	92.7	97.5
3) Ensemble classifier (using same data-set partition as [1])	95, 100, 97.5, 100, 100 (5-fold cross-validation)	93.02	97.5
4) Ensemble classifier (using random partition)	90.8, 95.5, 93.3, 93, 95.5	93.02	100

The relatively better and robust performance of the ensemble classifier can be attributed to two factors. One is that the ensemble classifier brings along several different classifiers for prediction, which makes it robust to outliers which might affect a specific classifier. The other major factor is that our models consider additional features such as X15 and X17. These features show the highest importance for the classification task, but they are not considered in the model by [1]. These features characterize the temperature-time curve within each charge cycle over the cycles from 70 to 100. As is evident, these features have a critical impact on predicting cycle life from earlier cycle data. The evolution of temperature from cycle 70 to 100 when the cell is at different voltage gives a predictable direction towards the increasing degradation of the cell. It should be noticed that, as early as up to first 100 cycles, most cells exhibit no detectable capacity fading (some even have increased capacities during very early cycles [9, 10]).

The results for the regression task are shown in Table 3 in terms of root mean squared error (RMSE) and mean percentage error in prediction. Two critical observations are standing out. First, Model 1 outperforms both Model 2 and Model 3 in all the runs with respect to either test error. As both Model 1 and Model 2 consider feature importance measures, hence by considering only important features, it helps the model from being over-fitted to the data, and having better performance in test data. Secondly, it can be observed that, in most runs, the SVR model achieves a lower percentage error than the elastic net model. The optimal hyperparameter used for SVR chose a kernel function with polynomial kernel of degree 2. That is, a nonlinear regression (polynomial of degree 2) between features and cycle life could predict the cycle life better in the unseen test data than a linear regression model. The best percentage error that SVR achieved on the primary test data is 9% and on the secondary test data is 10.9%, which is impressive, considering that the elastic net model could hardly achieve a percent error below 14% on any of these runs. Also, a similar percentage error on all runs indicates that the model does not overfit. The superior performance of our model can be

attributed to the inclusion of new within-charge-cycle temperature and voltage curve features.

Table 3. Regression prediction results

Runs	Feature selection model	Method	Train data		Primary test data		Secondary test data	
			RMSE	% error	RMSE	% error	RMSE	% error
1	Model 1	EN	110.8	11.4	196.7	14.1	165.3	**14.9**
		SVR	**100.9**	**10.1**	**185.2**	**14.1**	**157.6**	15.3
	Model 2	EN	**102.1**	10.1	199.0	14.2	175.1	16.3
		SVR	102.6	**9.2**	**193.7**	**12.5**	**166.9**	**14.4**
	Model 3	EN	99.8	10.1	205.5	15.0	**177.2**	16.5
		SVR	**92.0**	**9.1**	**190.6**	**13.6**	179.7	**15.8**
2	Model 1	EN	164.3	16.8	157.3	14.1	144.2	16.5
		SVR	**106.1**	**9.5**	**126.6**	**11.7**	**121.1**	**12.9**
	Model 2	EN	167.8	**13.6**	153.3	14.6	171.8	20.4
		SVR	**147.7**	14.2	**142.9**	**11.9**	**94.4**	**10.9**
	Model 3	EN	170.6	14.4	**157.5**	**15.2**	152.3	16.7
		SVR	**149.1**	**13.8**	181.7	15.7	**124.0**	**13.7**
3	Model 1	EN	180.0	16.8	147.7	13.0	148.9	15.7
		SVR	**166.6**	**12.9**	**123.1**	**9.0**	**119.3**	**11.5**
	Model 2	EN	**191.6**	16.1	**158.5**	14.0	147.2	15.9
		SVR	198.7	**12.6**	163.7	**11.6**	**112.6**	**11.6**
	Model 3	EN	**192.4**	17.3	**159.9**	14.1	147.5	15.9
		SVR	195.1	**12.2**	165.2	**11.0**	**109.7**	**11.5**
4	Model 1	EN	178.1	13.9	170.4	13.2	140.3	13.3
		SVR	**160.0**	**10.5**	**154.2**	**13.0**	**122.2**	**12.0**
	Model 2	EN	**176.8**	13.1	171.6	13.6	140.6	13.4
		SVR	183.6	**13.1**	**167.0**	**13.5**	**122.4**	**11.0**
	Model 3	EN	179.2	13.1	172.5	**14.6**	143.9	13.4
		SVR	**172.2**	**12.3**	**164.1**	14.9	**126.7**	**12.1**

5 CONCLUSIONS

In this study, we analyze the cycle life data of lithium-iron phosphate cells. Early cycle data (up to the first 100 cycles) and their features are carefully examined for building predictive models. It is observed that some of those suggested features (related to temperature and voltage curves), have very high feature importance scores with respect to both classification and regression tasks, which is aligned with the chemical and mechanical changes in the electrodes of lithium-iron battery over its life cycle. We suggest an EML method that combines several classifiers such as k-nearest neighbors, neural networks, support vector machines and decision tree-based classifiers, and this classifier provides more robust prediction over randomly partitioned datasets. For the regression task, a support vector regression model is suggested and compared with the elastic net regression model. It is observed that SVR outperforms elastic net in terms of percentage error over different dataset partitions by fitting nonlinear decision boundaries for the regression task.

REFERENCES

1. Kristen A Severson, Peter M Attia, Norman Jin, Nicholas Perkins, Benben Jiang, Zi Yang, Michael H Chen, Muratahan Aykol, Patrick K Herring, Dimitrios Fraggedakis, et al. Data-driven prediction of battery cycle life before capacity degradation. *Nature Energy*, 4(5):383-391, 2019.
2. HB Chenoweth. Soft failures and reliability. In *Annual Proceedings on Reliability and Maintainability Symposium*, pages 419-424. IEEE, 1990.
3. Christopher Hendricks, Nick Williard, Sony Mathew, and Michael Pecht. A failure modes, mechanisms, and effects analysis (FMMEA) of lithium-ion batteries. *Journal of Power Sources*, 297:113-120, 2015.
4. Guangming Liu, Minggao Ouyang, Languang Lu, Jianqiu Li, and Xuebing Han. Analysis of the heat generation of lithium-ion battery during charging and discharging considering different influencing factors. *Journal of Thermal Analysis and Calorimetry,* 116(2):1001-1010, 2014.
5. Jonas Hedman, David Nilebo, Elin Larsson Langhammer, and Fredrik Bjorefors. Fibre optic sensor for characterisation of lithium-ion batteries. *ChemSusChem,* 13(21):5731, 2020.
6. Guangsheng Zhang, Shanhai Ge, Terrence Xu, Xiao-Guang Yang, Hua Tian, and Chao-Yang Wang. Rapid self-heating and internal temperature sensing of lithium-ion batteries at low temperatures. *Electrochimica Acta*, 218:149-155, 2016.
7. Manh-Kien Tran and Michael Fowler. Sensor fault detection and isolation for degrading lithium-ion batteries in electric vehicles using parameter estimation with recursive least squares. *Batteries*, 6(1):1, 2020.
8. Fabian Pedregosa, Ga el Varoquaux, Alexandre Gramfort, Vincent Michel, Bertrand Thirion, Olivier Grisel, Mathieu Blondel, Peter Prettenhofer, Ron Weiss, Vincent Dubourg, et al. Scikit-learn: Machine learning in python. *Journal of Machine Learning Research*, 12:2825-2830, 2011.
9. Gang Ning, Bala Haran, and Branko N Popov. Capacity fade study of lithium-ion batteries cycled at high discharge rates. *Journal of Power Sources*, 117(1-2):160-169, 2003.
10. D Zhang, BS Haran, A Durairajan, Ralph E White, Y Podrazhansky, and Branko N Popov. Studies on capacity fade of lithium-ion batteries. *Journal of Power Sources*, 91(2):122-129, 2000.

BIOGRAPHIES

Ankan Mitra
School of Computing and Augmented Intelligence
Arizona State University, Tempe, Arizona, USA.

e-mail: amitra16@asu.edu

Ankan Mitra is a fourth year PhD student. His research interests include large-scale optimization, machine learning algorithms and applications.

Rong Pan, Ph.D.
School of Computing and Augmented Intelligence
Arizona State University, Tempe, Arizona, USA.

e-mail: rong.pan@asu.edu

Dr. Rong Pan is an Associate Professor of Industrial Engineering at ASU. His teaching and research interests are in the areas of statistical reliability modeling and data analysis. He is a senior member of ASQ, IIE and IEEE, and a lifetime member of SRE